XL CILAMCE
IBERO-LATIN AMERICAN CONGRESS ON COMPUTATIONAL METHODS IN ENGINEERING
NOVEMBER 11-14, 2019
Praiamar Natal Hotel & Convention Natal, RN-BRAZIL

RC BRIDGE FATIGUE RELIABILITY AND BRAZILIAN STRUCTURAL DESIGN ADEQUACY ASSESSMENT

Daniel Higor Leite Braz
Francisco Evangelista Junior, Ph.D.
danielhlbraz@gmail.com
fejr@unb.com.br
Structures and Civil Construction Postgraduate Program - University of Brasília
Campus Universitário Darcy Ribeiro, CEP 70910-90, Brasília-DF, Brazil

Abstract. The fatigue ultimate limit state is one of the most important considerations in the bridges' design. Sections' geometric characteristics, material properties and traffic are influential factors subjected to different levels of uncertainty. Hence, it is interesting to investigate the impact of their variabilities in the fatigue reliability of the reinforcements, here defined for four isostatic reinforced concrete (RC) bridges with two girders, through Monte Carlo simulations (MCS). It is also analyzed how adequate is the typical design approach. The results show that the extrapolated traffic has greater potential to penalize the reinforcements' fatigue performance than the Brazilian standard design vehicle TB-450. The importance of a more accurate technical control in the execution of bridges is highlighted, since the geometrical and material variabilities also contribute to the penalizations.

Keywords: Fatigue, bridges, design, reliability

1 Introduction

Fatigue is a form of failure that involves the formation and growth of cracks in a structural component, due to strains caused by time-varying loads. These loads have the potential to cause failure even when their maximum nominal intensities are inferior to the ultimate limit capacity of the structure (Murthy [1]). Every stress that fluctuates in time can cause fatigue failure, but the wider range stresses and those that have tension-compression alternations are more critical (Callister [2]; Dowling [3]).

This phenomenon is of particular interest to bridge engineering — it is an ultimate limit state of great importance as stated by Szerszen and Nowak [4] — since such structures are subjected to moving loads, with varying positions, which produce cyclic stresses. Specifically on the reinforcements, the fatigue failure occurs under a stress lower than the yield strength. This stress, however, must be higher than the respective fatigue limit. The type of steel, the geometry of deformations on the bars and their diameters, bending, occasional welding, anchorages and stress range are to be considered (Tilly [5]; Dowling [3]).

Deformations on rebars, used to obtain good bond between steel and concrete, produce stress concentration at their base, where the fatigue fractures are observed to initiate as shown by Rocha, Brühwiler e Nussbaumer [6] and Majumdar *et al* [7]. Welding, as well as bending, also reduces the strength. It is also verified that bars with larger widths have lower fatigue strength, as reported by the American Concrete Institute in ACI 215R-74 [8]. Concerning fatigue life, the higher the stress range, lower the required number of load cycles to cause failure. As noticed, the phenomenon is related to many aspects, making the design against fatigue a complex task. Even more when the uncertainties inherent to the phenomenon — such as the related to geometry, manufacturing quality, material properties and especially regarding traffic loads (Echard, Gayton and Bignonnet [9]) — are taken into account.

As these factors are prone to different levels of uncertainty, the evaluation of the structure probability of failure is fundamental. Thus, studies which consider the variabilities of the input parameters are interesting (Pan and Dias [10]). To date, research concerning traffic loads based on monitoring data (Nowak [11]; Crespo-Minguillón and Casas [12]; Nowak and Rakoczy [13]; Anitori, Casas and Ghosn [14]) and bridge fatigue reliability (Kwon and Frangopol [15]; Leander [16]) have shown the significance of probabilistic analysis and the constant need to adequate the standard's design procedure to what is in fact observed in the roadways.

In Brazil, the works of Ferreira, Nowak and Debs [17], Rossigali *et al*. [18] and Portela *et al*. [19] are the most relevant. The first verifies the reliability of reinforced and prestressed concrete bridges under the jurisdiction of the São Paulo Department of Transportation (DER-SP), with the goal to propose limits to truck weights. To do so, the authors propose length-weight limit equations for the trafficking vehicles of the studied roads. Rossigali *et al*. [18] compare the effects produced by the Brazilian design vehicle to the ones generated by a proposed live load model based in weigh-in-motion (WIM) data in short span roadway bridges (10 m to 40 m) with two lanes. Portela *et al*. [19] present WIM data of Fernão Dias highway (BR-381) — collected within a 13 months-period —, the main types of trucks, their characteristics and multiple presence scenarios. The data is meant to be a reliable dataset for a more appropriate Brazilian traffic load model.

The aforementioned, though assess the reliability of bridges for ultimate bending moments, they do not approach fatigue limit state on bridges. So, to this end, the fatigue reliability of the reinforcements of four models of isostatic reinforced concrete (RC) bridges with two girders will be evaluated through Monte Carlo Simulations (MCS). It is sought to investigate how adequate the typical design approach — which does not explicitly or sufficiently consider fluctuations on the sections' geometric features, in the materials and in traffic — is.

2 Background

To satisfy the proposed objectives, it is necessary to present the current Brazilian code procedures for RC bridges and the reliability technique applied in the present research.

2.1 Brazilian standard's design procedure for RC bridges

The intensity of the actions used on the design, F_d, are determined through ultimate normal combination of actions, given by:

$$F_d = \sum_{i=1}^{n} \gamma_g F_{gik} + \gamma_q \left(F_{q1k} + \sum_{j=2}^{m} \psi_{0j} F_{qjk} \right) \tag{1}$$

In which F_{gik} is the direct permanent action characteristic value *i*; F_{q1k} is the principal transient action characteristic value; F_{qjk} is the secondary transient action *j* characteristic value. According to ABNT NBR 8681:2003 [20], for bridges in general, the coefficients γ_g = 1.35 (1.00) and γ_q = 1.5 are used for clustered direct permanent and transient actions, respectively. The ψ_{0j} is a coefficient that multiplies the secondary transient actions.

To obtain the transient effects, the design vehicle TB-450 (Fig. 1) is used [21].

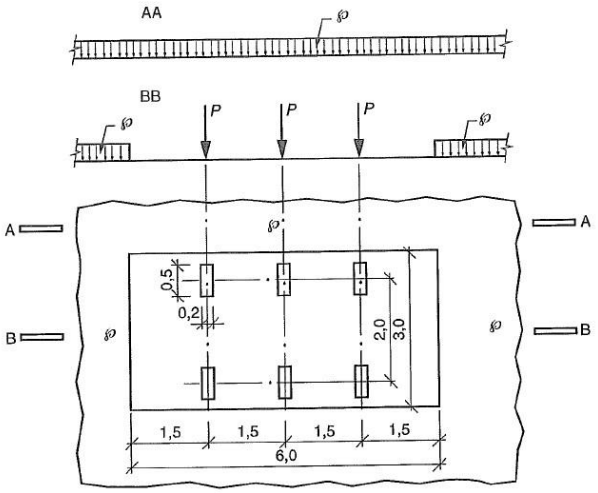

Figure 1. Brazilian design vehicle TB-450 [21]

Besides, the standard defines the following coefficients: *CIV* (vertical impact), *CNF* (number of lanes) and *CIA* (additional impact). The general impact coefficient is, hence, the product of the latter three which are calculated as shown ahead.

a) Vertical impact coefficient: enhances all vertical traffic loads. It is calculated by Eq. 2

$$CIV = \begin{cases} 1.35, \text{ for spans less than 10.0 m length} \\ 1 + 1.06\left(\dfrac{20}{L_{iv} + 50} \right), \text{ otherwise} \end{cases} \tag{2}$$

In which L_{iv} is the arithmetic mean of the spans, for continuous spans, or the cantilever length.

b) Number of lanes coefficient: enhances the traffic loads, being a function of the "*n*" integer number of traffic lanes to be loaded over a transversal continuous bridge deck (does not include safety lanes or shoulders).

$$CNF = 1 - 0.05(n-2) > 0.9 \tag{3}$$

c) Additional impact coefficient: enhances the actions at the regions of the structural joints and in the extremities of the structure. All sections located horizontally within 5.0 m from each side of the joint or structural discontinuity must be designed with actions increased by *CIA*, defined as follows.

$$CIA = \begin{cases} 1.25, \text{ for concrete or composite components} \\ 1.15, \text{ for steel components} \end{cases} \tag{4}$$

The coefficients above substitute the former from ABNT NBR 7187:2003 [22], given by Eq. 5:

$$\varphi = 1.4 - 0.007\ell \geq 1 \tag{5}$$

In which ℓ is the length of each theoretical span of the loaded component.

The fatigue verifications are contained in the chapter 23.5 "Ultimate limit state of fatigue" of the ABNT NBR 6118:2014 [23], which deals with medium and low intensity fatigue actions and number of repetitions up until 2 million cycles. Also, the Palmgren-Miner rule is considered valid for the combination of actions for a given load spectrum.

It is highlighted that the verification of fatigue can be accomplished by a unique magnitude of solicitation, $F_{d,ser}$, expressed by the frequent combination of actions in Eq. 6, though the phenomenon is controlled by the accumulation of damage produced by repeated loads.

$$F_{d,ser} = \sum_{i=1}^{m} F_{gik} + \psi_1 F_{q1k} + \sum_{j=2}^{n} \psi_{2j} F_{qjk} \tag{6}$$

In which F_{gik}, F_{q1k} and F_{qjk} are the same of Eq. 1.

It is interesting to notice that, although fatigue is an ultimate limit state (ULS), the code adopts a serviceability limit state (SLS) combination. For the corresponding combination, in the case of beams of roadway bridges, ψ_1 equals to 0.5 is used. For the calculus of the actions and stress verifications, a linear elastic model is assumed with ratio between the moduli of elasticity of steel and concrete $\alpha_e = 10$, in addition of $\gamma_f = 1.0$; $\gamma_c = 1.4$ and $\gamma_s = 1.0$.

For the rebars, the safety is assured if the maximum calculated variation of stress $\Delta\sigma$, for the frequent combination of actions, satisfies Eq. 7.

$$\gamma_f \Delta\sigma_{Ss} \leq \Delta f_{sd,fad} \tag{7}$$

The values of $\Delta f_{sd,fad}$ are presented in Table 1, for a number N of 2 million cycles, passive reinforcements and deformed bars with high adherence.

Table 1. Values of $\Delta f_{sd,fad}$ (MPa) [23]

Case	ϕ (mm)							
	10	12.5	16	20	22	25	32	40
Straight bars or bended with $D \geq 25\ \phi$	190	190	190	185	180	175	165	150
Straight bars or bended with: $D < 25\ \phi$ $D = 5\ \phi < 20$ mm $D = 8\ \phi \geq 20$ mm	105	105	105	105	100	95	90	85

The function of steel fatigue strength, represented in logarithmic scale in Fig. 2, consists in line segments of the form $(\Delta f_{sd,fad})^m \times N$ = constant. For the considered bars, $N^* = 10^6$, $k_1 = 5$ and $k_2 = 9$.

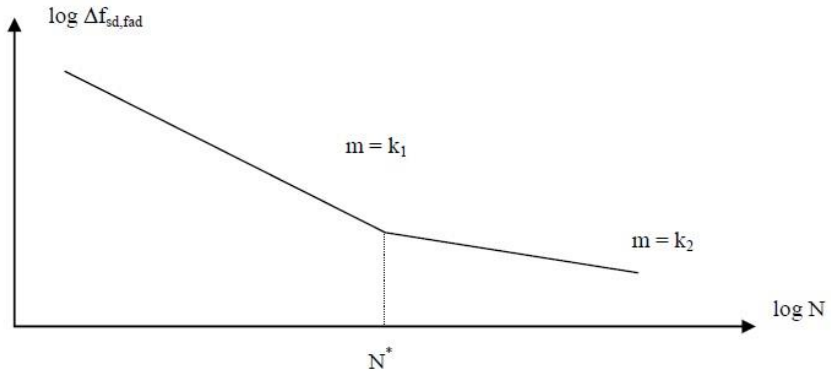

Figure 2. Standard shape of the S-N curves of the steel fatigue strength [23].

2.2 Monte Carlo Simulation (MCS)

For structural reliability assessment, Monte Carlo simulation (MCS) consists in a three stages procedure, conforming to Pan & Dias [10]: (1) generation of n_{MC} values of x_i for the chosen random variable (RV), in accordance to the underlying probability density function (PDF); (2) determination of the corresponding value of the reliability function G for every value of x_i and (3) post-calculus of the probability of failure P_f or the statistical moments. P_f can be obtained by Eq. 8, where I is a function that computes the number of times of $G(x_i) < 0$.

$$P_f = \frac{1}{n_{MC}} \sum_{i=1}^{n_{MC}} I\left[G\left(x_i\right) < 0\right] \tag{8}$$

Though its numerous attractive features, the most important being how easy it is to check the failure criterion even in complex systems, MCS may have the flip side of demanding intense computational effort [24].

Once establish the Pf, the equivalent reliability index β_{MC} is calculated by Eq. 9.

$$\beta_{MC} = -\Phi^{-1}\left(P_f\right) \tag{9}$$

In which Φ^{-1} is the inverse cumulative density function (CDF) of the standard normal distribution.

3 Studied models and Reliability functions

3.1 Studied models

The models, also used in Ferreira [25] and Ferreira, Nowak and Debs [17], are four isostatic RC bridges with two girders. They are simply supported (SA), of large (TL) or narrow deck (TE), with 20 (V20) or 10 m (V10) spans and with one (TR1) or two (TR2) transverse beams — which have 80% of the respective girder height. The general configuration is presented on Fig. 3.

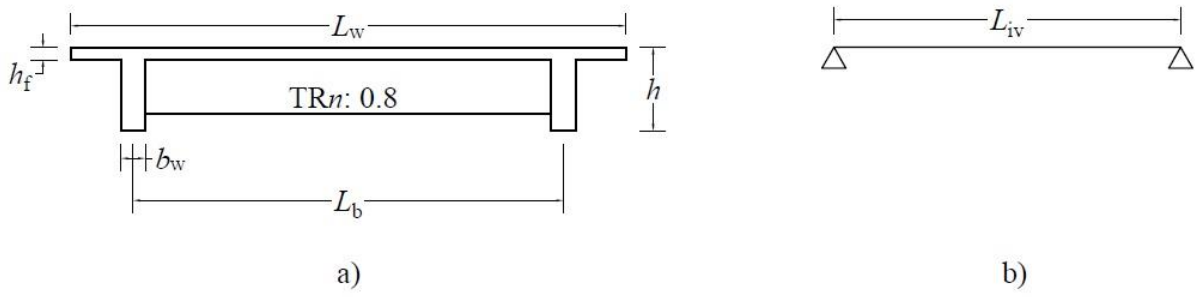

a) b)

Figure 3. Bridge models configuration: a) cross section; b) longitudinal aspect.

In which, L_{iv} is equal to the span length; L_w is the transverse bridge width; L_b is the distance between the girders' axis; h is the girders' height; h_f is the deck height; b_w is the web width; n is the number of transverse beams. For each model, the values of such parameters are presented in Table 2. The values of the effective width of flanges (b_f) are also shown.

Table 2. Geometric parameters of each model

Model	L_{iv} (m)	L_w (m)	L_b (m)	h (cm)	h_f (cm)	b_w (cm)	b_f (cm)	n
SA TE V10 TR2	10	8	6	120	18	35	207	2
SA TE V20 TR2	20	8	6	200	18	45	312	2
SA TL V10 TR1	10	12	8	120	25	40	240	1
SA TL V20 TR2	20	12	8	200	25	45	442	2

The actions where determined by Ferreira [25] through modeling in Structural Analysis Program v. 9.0 (STRAP), where the orthogonal girders were conceived as bar elements and the deck, as plate elements. The transverse beams were considered in the support areas and in intermediate positions to those and the edges of the girders.

To calculate the bending moments, only the effects of the vertical actions were contemplated (self-weight of the concrete components and the asphalt pavement and moving loads) in the main structure. Wind, temperature, breaking and others were not included. In Table 3, the impact coefficients used at the time and the ones achieved by the current procedure (Eq. 2 to 4).

Table 3. Transient actions' impact coefficients

Model	$\varphi_{\text{NBR 7187}}$	L_{iv} (m)	CIV	CNF	CIA	$\phi_{\text{NBR 7188}}$
SA TE V10 TR2	1.33	10.00	1.35	1.00	1.00	1.35
SA TE V20 TR2	1.26	20.00	1.30	1.00	1.00	1.30
SA TL V10 TR1	1.33	10.00	1.35	0.95	1.00	1.29
SA TL V20 TR2	1.26	20.00	1.30	0.95	1.00	1.24

In Table 4, the bending moments M_g (permanent) and M_q (transient, from the Brazilian standard design vehicle TB-450), including the $M_{q,corr}$ (transient, produced by TB-450, but corrected by the up-to-date $\phi_{\text{NBR 7188}}$ impact coefficient).

Table 4. Bending moments and geometric characteristics

Model	M_g (kNm)	M_q (kNm)	$M_{q,corr}$ (kNm)	h (cm)	d_{est} (cm)	h_f (cm)	b_w (cm)	b_f (cm)
SA TE V10 TR2	518.7	877.7	893.1	120.0	108.0	18.0	35.00	207.0
SA TE V20 TR2	2727.9	2423.2	2505.6	200.0	180.0	18.0	45.00	312.0
SA TL V10 TR1	797.6	1074.9	1039.1	120.0	108.0	25.0	40.00	240.0
SA TL V20 TR2	3995.5	3075.6	3021.2	200.0	180.0	25.0	45.00	442.0

3.2 Fatigue reliability of the reinforcements

The reliability assessment requires the definition of the limit state function G. By its turn, G demands the determination of the neutral axis x_{II} and moment of inertia I_{II} of the cracked concrete section. The first is given by:

$$x_{II} = \frac{-a_2 \pm \sqrt{a_2^2 - 4a_1a_3}}{2a_1} \tag{10}$$

In which

$$a_1 = b_w$$
$$a_2 = 2\left[h_f\left(b_f - b_w\right) + \alpha_e\left(A_s + A_s^{'}\right)\right]$$
$$a_3 = -\left[h_f^2\left(b_f - b_w\right) + 2\alpha_e\left(A_s d + A_s^{'} d^{'}\right)\right] \quad (10.a, b, c)$$

In which b_w, b_f and h_f were previously defined. A_s is the cross sectional area of reinforcement under tension; A'_s is the cross sectional area of reinforcement under compression for the applied moment; d is the effective depth of the cross-section; d' is the effective depth of the cross-section for the rebars under compression for the applied moment.

And the moment of inertia:

$$I_{II} = \frac{b_f h_f^3}{12} + b_f h_f\left(x_{II} - \frac{h_f}{2}\right)^2 + \frac{b_w\left(x_{II} - h_f\right)^3}{3} + \alpha_e\left[A_s\left(d - x_{II}\right)^2 + A_s^{'}\left(d^{'} - x_{II}\right)^2\right] \quad (11)$$

From the above, the maximum stress $\sigma_{max,s}$ is calculated Eq. 12 using the maximum moment $M_{d,fad,max}$ of the combination in Eq. 6:

$$\sigma_{max,s} = \frac{\alpha_e M_{d,fad,max}\left(d - x_{II}\right)}{I_{II}} \quad (12)$$

And the $\sigma_{min,s}$, as shown in Eq. 13, for the minimum bending moment $M_{d,fad,min}$:

$$\sigma_{min,s} = \frac{\alpha_e M_{d,fad,min}\left(d - x_{II}\right)}{I_{II}} \quad (13)$$

The reliability function G is, therefore, given by Eq. 14, where $\Delta\sigma_s/\Delta f_{sd,fad}$ is the so called fatigue factor.

$$G = 1 - \frac{\Delta\sigma_s}{\Delta f_{sd,fad}} = 1 - \frac{\alpha_e \Delta M_{d,fad}\left(d - x_{II}\right)/I_{II}}{\Delta f_{sd,fad}} \quad (14)$$

The geometric characteristics of the girders were treated as RV. In Table 5, their means and coefficients of variation (CV). These variabilities allude to eventual errors in the execution in situ.

Table 5. Statistical parameters of the RV

Symbol	μ	CV	Distribuition
h_f	h_f	$0.5/h_f$	normal
h	h	$0.5/h$	normal
b_f	b_f	-	-
b_w	$1.01b_w$	0.04	normal
d	$0.99d$	0.04	normal
f_{ck} (MPa) = 25	28	0.093	normal
E_s (MPa)	210000	0.06	lognormal

The traffic is also a RV. The isolated short truck *3S3* model, on Fig. 4, is used. As Ferreira, Nowak & Debs [17] stated, this configuration is the most critical for the prediction of the maximum efforts in the evaluated structures and its mean maximum gross weight (1009.1 kN) was obtained through extrapolation for a design life of 50 years, according to the following procedure.

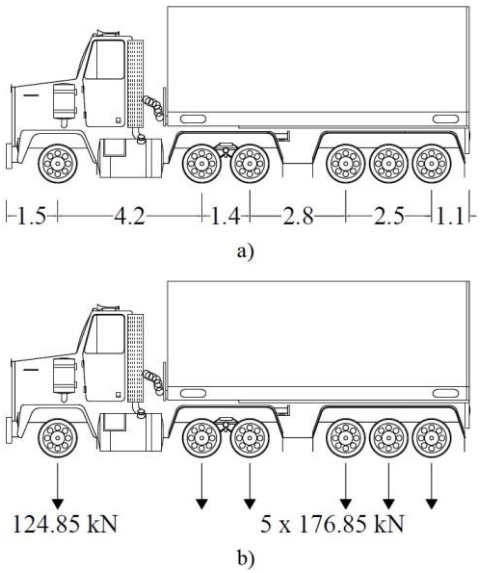

Figure 4. *3S3* short truck. a) axle spacing in meters; b) axle loads.

To obtain the mean maximum gross vehicle weight (*GVW*), the researchers plotted the weight data on normal probability paper. Then, for an average daily truck traffic (*ADTT*) of 364 *3S3* trucks, the authors calculated the corresponding total number of trucks (*N*) and the standard normal variable $z = -\Phi^{-1}(1/N)$. In Table 6, the *z* values for every time period *T*.

Table 6. Values of *z* for the considered time periods - ADTT = 364

T	N_v	*z*
1 day	364	2.78
1 month	10920	3.74
2 months	21840	3.91
1 year	132860	4.33
5 years	664300	4.67
50 years	6643000	5.12

Once defined, it is possible to extrapolate the *GVW* data for a chosen time. By admitting a normal distribution for the weights, a straight line is drawn from the upper tail, considering the 10% heaviest trucks, according to Ferreira [25]. In Fig. 5 the performed extrapolation for the *3S3* truck is shown. The axle loads are determined by multiplying the *GVW* times the respective permitted axle load.

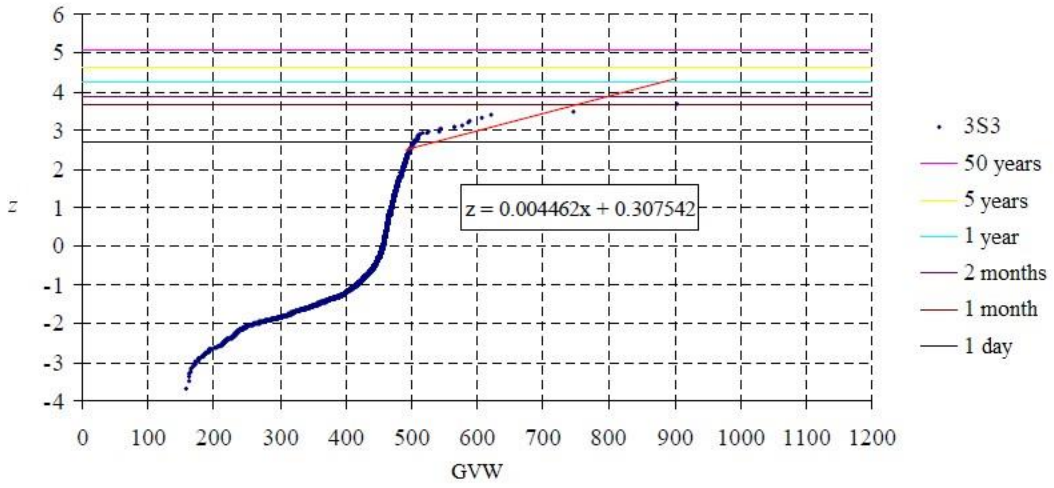

Figure 5. Extrapolation of the *3S3* short truck, as performed by Ferreira [25].

The standard deviation of the GVW is the inverse of the angular coefficient of the extrapolation line, hence 224.1. Therefore, the CV is 0.222 (calculated from 224.1/1009.1). Since the distance between axes and the weight per axis are deterministic, this is also the CV of the moments M_{3S3} produced by the *3S3* trucks, as presented in Table 7.

Table 7. Bending moments obtained by the isolated *3S3* short truck

Model	M_{3S3} (kNm)	CV
SA TE V10 TR2	1042.8	0.222
SA TE V20 TR2	2892.6	0.222
SA TL V10 TR1	1192.3	0.222
SA TL V20 TR2	3379.4	0.222

Along with the abovementioned, the fatigue strength $\Delta f_{sd,fad}$ will be RV. A Weibull distribution, with the following PDF, is assumed.

$$f\left(x \mid a,b\right) = \frac{b}{a}\left(\frac{x}{a}\right)^{b-1} \exp\left(\frac{-x}{a}\right)^{b} \tag{15}$$

In which a is the scale parameter and b, the shape. The relations to the mean μ and variance σ^2 are expressed ahead, where Γ stands for the gamma function.

$$\mu = a\left[\Gamma\left(1+b^{-1}\right)\right] \tag{16}$$

$$\sigma^2 = a^2\left[\Gamma\left(1+2b^{-1}\right) - \Gamma\left(1+b^{-1}\right)^2\right] \tag{17}$$

According to Kwon and Frangopol [15], this is one of the possible distributions for the estimative of stress range. As stated by Dowling [3], a typical coefficient of variation for fatigue strength is 10%. Hence these distribution and CV will be adopted in the further analysis.

3.3 Brazilian design approach adequacy

To verify the adequacy of the typical design approach, the reliability function H is proposed.

$$H = G - \Omega \tag{18}$$

Where Ω stands for the design-approach generated value analogue to Eq. 14. The values $H < 0$, contributors to the $P_{f,H}$, inform how many times the fatigue factor calculated by the typical design approach is lower than the one obtained from the comprehension of the influential factors' variability on the reinforcements' fatigue.

4 Results and Discussion

In Table 8, the current design results and the fatigue factor of the rebars. The TB-450 was used. It is noticed that all models satisfy the condition given by Eq. 7.

Table 8. Design and fatigue factor - Current design approach analysis

Model	$\Delta M_{d,fad}$ (kNm)	A_s (cm^2)	n°	ϕ (mm)	$\Delta f_{sd,fad}$ (MPa)	d (cm)	Ω
SA TE V10 TR2	446.55	45.33	37	12.5	190.00	109.40	0.4960
SA TE V20 TR2	1252.80	99.21	32	20.0	185.00	189.75	0.6231
SA TL V10 TR1	519.55	58.56	48	12.5	190.00	108.27	0.5414
SA TL V20 TR2	1510.60	132.34	27	25.0	180.00	187.53	0.6331

Ahead, the probabilistic results for 2 million MCS. The values of $\Delta f_{sd,fad}$ presented in Table 8 are the means of the Weibull distributions. The scale and shape parameters calculated are shown in Table 9. Once known, it is possible to generate values of $\Delta f_{sd,fad}$ for the underlying PDF.

Table 9. Shape b and scale a parameters of $\Delta f_{sd,fad}$ for each model

Model	μ	CV	b	a
SA TE V10 TR2	190	0.10	12.013	198.263
SA TE V20 TR2	185	0.10	12.013	193.045
SA TL V10 TR1	190	0.10	12.013	198.263
SA TL V20 TR2	180	0.10	12.013	187.828

In Table 10, the statistical moments, β and P_f of G and bias factor λ (the ratio between average of G and Ω). The models satisfy the condition given by Eq. 7.

Table 10. Mean μ, CV, β and P_f of G for each model

Model	μ_G	CV	$P_{f,G}$	β_G	λ
SA TE V10 TR2	0.4006	0.3809	0.0111	2.2864	0.8078
SA TE V20 TR2	0.5557	0.2035	0.0003	3.4008	0.8918
SA TL V10 TR1	0.4680	0.2892	0.0028	2.7667	0.8645
SA TL V20 TR2	0.5931	0.1747	0.0001	3.6552	0.9369

In Table 11, the statistical moments and P_f of H.

Table 11. Mean μ, CV and P_f of H for each model

Model	μ_H	CV	$P_{f,H}$
SA TE V10 TR2	-0.0953	1.6006	0.7297
SA TE V20 TR2	-0.0674	1.6763	0.7195
SA TL V10 TR1	-0.0733	1.8453	0.6988
SA TL V20 TR2	-0.0400	2.5919	0.6372

In Fig. 6 the *G* histograms for each model and the respective Normal Distribution Adjust Curve.

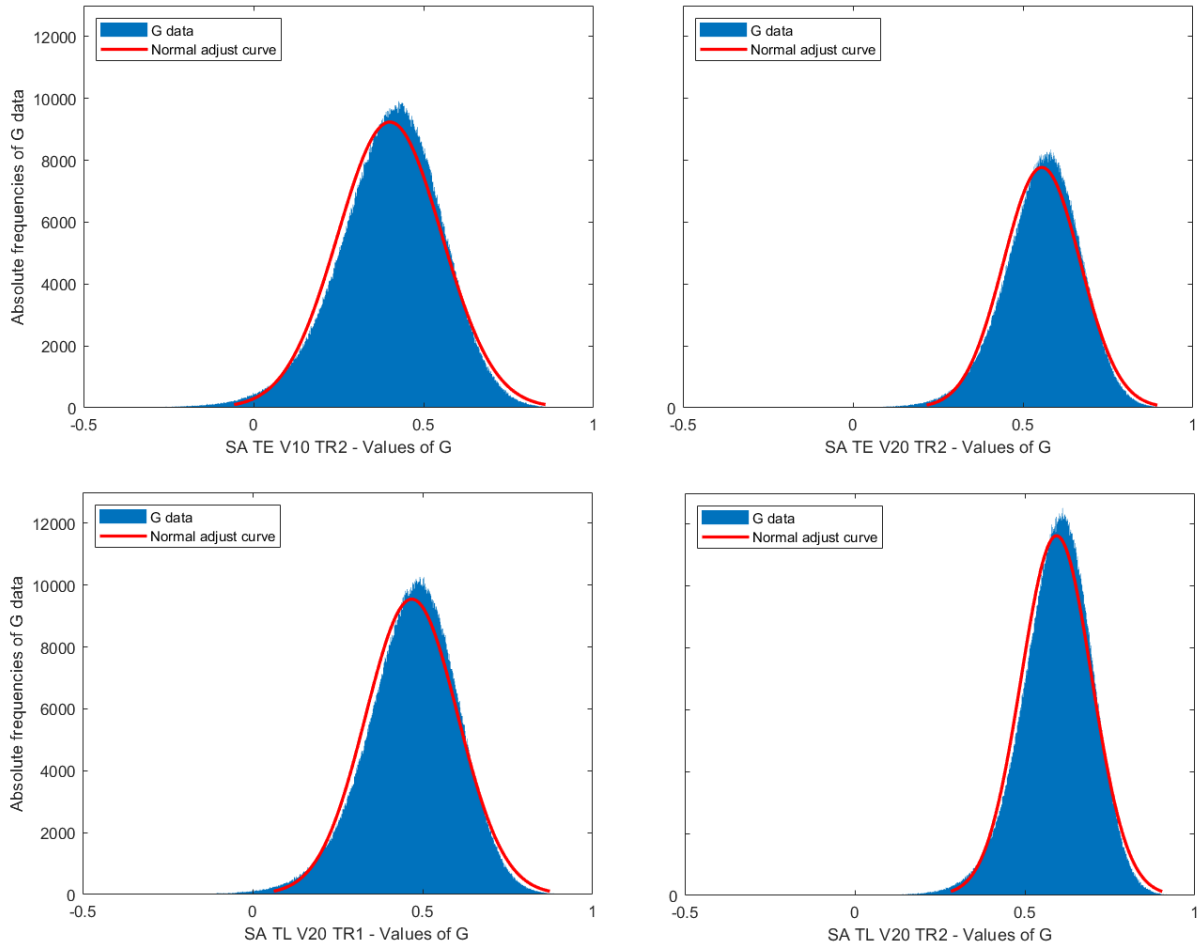

Figure 6. Histograms of *G* for each model and the respective Normal Adjust curves [26].

All λ of *G* are inferior to unity. The $P_{f,H}$ were higher than 60%. When deviations on the fatigue strength of the rebars are comprehended, in addition to the ones in geometry, materials and traffic, the performance is penalized. For example, the SA TE V10 TR2 computed almost 73% of events where the uncertainty-added scenarios' fatigue factors were higher than the ones produced by the current design approach. This indicates that on the majority of the events, the Brazilian standards-based procedure did not produced conservative results.

5 Conclusions

Set the importance of bridges, the fatigue performance of the rebars of four models of isostatic RC bridges with two girders were evaluated through MCS. Specifically, it was sought to investigate the importance of the influential factors' variabilities on the phenomenon and how adequate is the typical design approach in front of the intrinsic uncertainties of geometry, materials and traffic.

When compared to the Ω results, it was verified that the mean values of *G* were inferior, thus the performance of the rebars were lower than the ones generated through the design procedure. The decreases, also expressed by the high probabilities of failure of *H*, indicate that the extrapolated traffic has greater potential to penalize the girders' rebars' fatigue performance than the design vehicle TB-450, and are also a stimuli to a broaden surveillance at the Brazilian roadways regarding trucks' weight. This is an additional indicative to the inadequacy of the current standard truck in face of the current traffic, also highlighted by Rossigali *et al* [18].

As Anitori, Casas & Ghosn [14] point out, the typical bridge design, the evaluation processes and the refined reliability analysis are very sensible to the traffic loads from the roadway bridges. In the present work, it is noticed that the fatigue of the rebars are too. Better technical control in the execution of the structures and manufacturing quality are also emphasized, since the variabilities in geometry and materials also contribute to lower performances.

Acknowledgements

We would like to thank the Structures and Civil Construction Postgraduate Program of the University of Brasília (PECC-UnB) for the support to the present research.

References

[1] MURTHY, A. Ramachandra et al. Fatigue behaviour of damaged RC beams strengthened with ultra high performance fibre reinforced concrete. International Journal of Fatigue, [s.l.], v. 116, p.659-668, nov. 2018. Elsevier BV. http://dx.doi.org/10.1016/j.ijfatigue.2018.06.046.
[2] CALLISTER, William D. Jr. Materials Science and Engineering: An Introduction. 7. ed. York, PA: John Wiley & Sons, Inc., 2007.
[3] DOWLING, Norman E. Mechanical Behavior of Materials: Engineering Methods for Deformation, Fracture, and Fatigue. 4. ed. Essex, England: Pearson Education Limited, 2013. 954 p. (Pearson International Edition). Contributions by Katakam Siva Prasad and R. Narayanasamy.
[4] SZERSZEN, Maria; NOWAK, Andrzej. Fatigue Evaluation of Steel and Concrete Bridges. Transportation Research Record: Journal of the Transportation Research Board, [s.l.], v. 1696, p.73-80, jan. 2000. SAGE Publications. http://dx.doi.org/10.3141/1696-10.
[5] TILLY, G. P. Fatigue of steel reinforcement bars in concrete: a review. Fatigue & Fracture of Engineering Materials and Structures, [s.l.], v. 2, n. 3, p.251-268, out. 1979. Wiley. http://dx.doi.org/10.1111/j.1460-2695.1979.tb01084.x.
[6] ROCHA, Marina; BRÜHWILER, Eugen; NUSSBAUMER, Alain. Geometrical and Material Characterization of Quenched and Self-Tempered Steel Reinforcement Bars. Journal of Materials In Civil Engineering, [s.l.], v. 28, n. 6, jun. 2016. American Society of Civil Engineers (ASCE). http://dx.doi.org/10.1061/(asce)mt.1943-5533.0001355.
[7] MAJUMDAR, Shrabani et al. Optimum Rib Design in TMT Rebars to Enhance Fatigue Life While Retaining Bond Strength. Journal of Materials in Civil Engineering, [s.l.], v. 30, n. 3, mar. 2018. American Society of Civil Engineers (ASCE). http://dx.doi.org/10.1061/(asce)mt.1943-5533.0002173.
[8] AMERICAN CONCRETE INSTITUTE. ACI 215R-74: Considerations for Design of Concrete Structures Subjected to Fatigue Loading. Michigan, 1997.
[9] ECHARD, B.; GAYTON, N.; BIGNONNET, A. A reliability analysis method for fatigue design. International Journal of Fatigue, [s.l.], v. 59, p.292-300, fev. 2014. Elsevier BV. http://dx.doi.org/10.1016/j.ijfatigue.2013.08.004.
[10] PAN, Qiujing; DIAS, Daniel. An efficient reliability method combining adaptive Support Vector Machine and Monte Carlo Simulation. Structural Safety, [s.l.], v. 67, p.85-95, jul. 2017. Elsevier BV. http://dx.doi.org/10.1016/j.strusafe.2017.04.006.
[11] NOWAK, Andrzej S. Live load model for highway bridges. Structural Safety, [s.l.], v. 13, n. 1-2, p.53-66, dez. 1993. Elsevier BV. http://dx.doi.org/10.1016/0167-4730(93)90048-6.
[12] CRESPO-MINGUILLÓN, César; CASAS, Juan R. A comprehensive traffic load model for bridge safety checking. Structural Safety, [s.l.], v. 19, n. 4, p.339-359, jan. 1997. Elsevier BV. http://dx.doi.org/10.1016/s0167-4730(97)00016-7.
[13] NOWAK, Andrzej S.; RAKOCZY, Przemyslaw. WIM-based live load for bridges. Ksce Journal of Civil Engineering, [s.l.], v. 17, n. 3, p.568-574, abr. 2013. Springer Nature. http://dx.doi.org/10.1007/s12205-013-0602-8.
[14] ANITORI, Giorgio; CASAS, Joan R.; GHOSN, Michel. WIM-Based Live-Load Model for Advanced Analysis of Simply Supported Short- and Medium-Span Highway Bridges.

[15] KWON, Kihyon; FRANGOPOL, Dan M. Bridge fatigue reliability assessment using probability density functions of equivalent stress range based on field monitoring data. International Journal of Fatigue, [s.l.], v. 32, n. 8, p.1221-1232, ago. 2010. Elsevier BV. http://dx.doi.org/10.1016/j.ijfatigue.2010.01.002.
[16] LEANDER, John. Reliability evaluation of the Eurocode model for fatigue assessment of steel bridges. Journal of Constructional Steel Research, [s.l.], v. 141, p.1-8, fev. 2018. Elsevier BV. http://dx.doi.org/10.1016/j.jcsr.2017.11.010.
[17] FERREIRA, L. M.; NOWAK, A. S.; DEBS, M. K. El. Desenvolvimento de equações para a limitação do peso de veículos de carga em pontes de concreto através da teoria de confiabilidade. Revista Ibracon de Estruturas e Materiais, [s.l.], v. 1, n. 4, p.421-450, dez. 2008. FapUNIFESP (SciELO). http://dx.doi.org/10.1590/s1983-41952008000400005.
[18] ROSSIGALI, C. E. et al. Towards actual Brazilian traffic load models for short span highway bridges. Revista Ibracon de Estruturas e Materiais, [s.l.], v. 8, n. 2, p.124-139, abr. 2015. FapUNIFESP (SciELO). http://dx.doi.org/10.1590/s1983-41952015000200005.
[19] PORTELA, E. L. et al. Single and multiple presence statistics for bridge live load based on weigh-in-motion data. Revista Ibracon de Estruturas e Materiais, [s.l.], v. 10, n. 6, p.1163-1173, nov. 2017. FapUNIFESP (SciELO). http://dx.doi.org/10.1590/s1983-41952017000600002.
[20] ASSOCIAÇÃO BRASILEIRA DE NORMAS TÉCNICAS. NBR 8681: Ações e segurança nas estruturas - Procedimento. Rio de Janeiro, 2003.
[21] ASSOCIAÇÃO BRASILEIRA DE NORMAS TÉCNICAS. NBR 7188: Carga móvel rodoviária e de pedestre em pontes, viadutos, passarelas e outras estruturas. 2 ed. Rio de Janeiro, 2013.
[22] ASSOCIAÇÃO BRASILEIRA DE NORMAS TÉCNICAS. NBR 7187: Projeto de pontes de concreto armado e de concreto protendido - Procedimento. Rio de Janeiro, 2003.
[23] ASSOCIAÇÃO BRASILEIRA DE NORMAS TÉCNICAS. NBR 6118: Projeto de estruturas de concreto - Procedimento. 3 ed. Rio de Janeiro, 2014.
[24] NAESS, A.; LEIRA, B.J.; BATSEVYCH, O. System reliability analysis by enhanced Monte Carlo simulation. Structural Safety, [s.l.], v. 31, n. 5, p.349-355, set. 2009. Elsevier BV. http://dx.doi.org/10.1016/j.strusafe.2009.02.004.
[25] FERREIRA, Luciano Maldonado. Aplicação da teoria da confiabilidade na obtenção de limites para o peso de veículos de carga em pontes de concreto. 2006. 190 f. Tese (Doutorado) - Curso de Engenharia de Estruturas, Programa de Pós-graduação em Engenharia Civil, Escola de Engenharia de São Carlos da Universidade de São Paulo, São Carlos, 2006.
[26] MATLAB R2019a: MathWorks, 2019.